UnSegMedGAT: Unsupervised Medical Image Segmentation using Graph Attention Networks Clustering

A. Mudit Adityaja * ,Saurabh J. Shigwan† and Nitin Kumar†

*Shiv Nadar School, Noida, India

† Shiv Nadar Institution of Eminence, Delhi NCR, India

mudit.adityaja@sns.edu.in,{saurabh.shigwan, nitin.kumar}@snu.edu.in

Abstract—The data-intensive nature of supervised classification drives the interest of the researchers towards unsupervised approaches, especially for problems such as medical image segmentation, where labeled data is scarce. Building on the recent advancements of Vision transformers (ViT) in computer vision, we propose an unsupervised segmentation framework using a pre-trained Dino-ViT [1]. In the proposed method, we leverage the inherent graph structure within the image to realize a significant performance gain for segmentation in medical images. For this, we introduce a modularity-based loss function coupled with a Graph Attention Network (GAT) to effectively capture the inherent graph topology within the image. Our method achieves state-of-the-art performance, even significantly surpassing or matching that of existing (semi)supervised technique such as MedSAM [2] which is a *Segment Anything Model* in medical images. We demonstrate this using two challenging medical image datasets ISIC-2018 [3] and CVC-ColonDB [4]. This work underscores the potential of unsupervised approaches in advancing medical image analysis in scenarios where labeled data is scarce. The github repository of the code is available on https://github.com/mudit-adityaja/UnSegMedGAT.

Index Terms—Medical image segmentation, Unsupervised method, Graph attention network, Pre-trained model

I. INTRODUCTION

Image segmentation is a crucial downstream task in healthcare and computer vision, with many methods developed primarily using supervised deep learning techniques that require extensive annotated data. This is particularly challenging in medical image segmentation due to the difficulty of obtaining such annotated data. We propose a novel method in unsupervised image segmentation, an area that has been comparatively less explored. Convolutional Neural Networks (CNNs) have become popular for image segmentation, with architectures like UNet [5], SegNet [6], and DeepLab [7] effectively extracting features from input images. However, these supervised methods depend on labeled datasets, which are resource-intensive to create and often limited by privacy issues, particularly in healthcare. Additionally, models trained on specific datasets may not generalize well to new data due to variations in imaging protocols and subjects. The MedSAM model [2], a recent advancement in medical image segmentatin, uses a vision transformer (ViT) [1] architecture and is trained on a large dataset to improve generalization across diverse anatomical structures and conditions. Despite its advancements, MedSAM struggles with modality imbalance, leading to bias towards majority classes. Moreover, it has primarily been tested on cancer data only. Recent approaches combining ViT with Graph Convolution Networks (GCN) [8] have shown promising results [9], [10], [11] in computer vision. In our work, we utilize a Dino-ViT [1] model to extract pretrained features from images and create a complete graph structure from these features. We prune edges based on features dissimilarity, and optimize segmentation clusters using Modularity loss [12] in an unsupervised manner. The contribution of this paper can be summarized below:

- We propose a novel unsupervised approach in medical imaging domain by incorporating modularity [13] and attention mechanism [14] based criteria. This approach leverages features extracted from a pre-trained Vision Transformer [1] along with the intrinsic graph structure of the images for efficient image segmentation.
- We deploy an ensemble of multi-level Graph attention networks [15] for underlying graph clustering required for effective image segmentation.
- Our method, *UnSegMedGAT*, demonstrates superior performance compared to other state-of-the-art techniques, including MedSAM, on the ISIC-2018 dataset. Additionally, it significantly surpasses existing unsupervised methods on the CVC-ColonDB dataset.

II. PROPOSED METHOD

Our approach starts with an input image of dimensions $s \times t$ and d channels, which is processed through a pre-trained small vision transformer (ViT) [1] without any fine-tuning. The transformer segments the image into patches of size $p \times p$, yielding a total of $n = st/p^2$ patches. This is followed by extracting the internal representation for each patch from the key layer features of the final transformer block, known for its strong performance across various tasks. This results in feature vectors f of size $(st/p^2) \times C_{in}$, where C_{in} denotes the token embedding dimension for each image patch. Next, we construct the graph $\mathcal{G}$ with nodes representing corresponding feature vectors f, that captures neighborhood relationships through a correlation matrix A , defined as follows:

$$A = ff^{T} \cdot \left(ff^{T} > \tau \right) \in \mathbb{R}^{\frac{st}{p^2} \times \frac{st}{p^2}}, \quad (1)$$
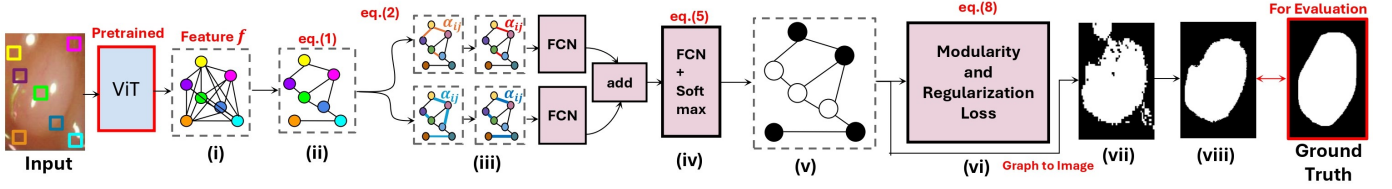
Fig. 1. UnSegMedGAT Pipeline: we i) extract features f of all (overlapping) image patches using vision transformer (ViT) and formulate a (complete) Graph $\mathcal{G}$ (few nodes shown, for illustration, in the same color as image patch windows), ii) then apply similarity (normalized ff^T) threshold to select important edges in $\mathcal{G}$, iii) aggregate and normalize features in GAT, darker node colors represent aggregation per series of GATs , iv) apply a fully connected network (FCN) with softmax activation to finally obtain node level clusters. vi) The modularity and regularization-based loss is finally used to train the model. vii-viii) At inference, edge refinement [16] is used over the predicted mask.

In this equation, the entries of the adjacency matrix A, denoted as A_{ij}, take values in $(0, 1)$, with $\tau \in (0, 1)$ being a user-defined parameter tailored to the specific dataset. The application of equation (1) on the normalized node features f of $\mathcal{G}$ is illustrated in Fig. 1 (ii).

In case of Graph Attention Networks (GAT), we leverage an attention mechanism to dynamically weigh the importance of different nodes and their connections during the learning process. This leads to a significant improvement over traditional graph convolutional networks (GCNs), which treat all neighbors equally [8].

Each node i in the graph is represented by a feature vector $\mathbf{h}_i \in \mathbb{R}^F$, where F is the number of features. The attention coefficients α_{ij} between nodes i and j are computed using a shared attention mechanism [15] as follows:

$$\alpha_{ij} = \frac{\exp(\text{LeakyReLU}(\mathbf{a}^\top[\mathbf{W}\mathbf{h}_i||\mathbf{W}\mathbf{h}_j]))}{\sum_{k \in \mathcal{N}(i)} \exp(\text{LeakyReLU}(\mathbf{a}^\top[\mathbf{W}\mathbf{h}_i||\mathbf{W}\mathbf{h}_k]))} \quad (2)$$

Here $\mathbf{W}$ is a learnable weight matrix, $\mathbf{a}$ is a learnable parameter vector, $||$ denotes concatenation, $\mathcal{N}(i)$ denotes the neighbors of node i.

The output feature vector for each node i after applying the attention mechanism is computed as follows:

$$\mathbf{h}_i' = \sigma\left(\sum_{j \in \mathcal{N}(i)} \alpha_{ij}\mathbf{W}\mathbf{h}_j\right) \quad (3)$$

Where σ is a non-linear activation function (e.g., ReLU). The sum aggregates the features of neighboring nodes weighted by their respective attention coefficients.

A. Multi-Head Attention

To enhance the model's expressiveness, GATs employ multi-head attention [14]. The final output of the ith node can be written as concatenation of outputs from individual heads:

$$\mathbf{H}_i' = ||_{z=1}^{Z}\left(\sigma\left(\sum_{j \in \mathcal{N}(i)} \alpha_{ij}^z\mathbf{W}^z\mathbf{h}_j\right)\right) \quad (4)$$

Here, Z represents the number of attention heads, and each head has its own weight matrix, allowing for diverse representations. $||$ denotes concatenation operator.

B. UnSegMedGAT model

We employ R parallel series of Graph Attention Networks (GATs) where any r^{th} row consists of t_r sequential Graph Attention layers, producing m_r output dimensions. This allows us to capture diverse set of features at each layer. The features are subsequently aggregated through two fully connected network (FCN) layers as mentioned in equation (5): (i)The first FCN projects the m_r dimensions to M dimensions. (ii)The outputs from all parallel GAT layers are summed, followed by a second FCN that transforms the aggregated features from M dimensions to k dimensions, yielding the final cluster assignment $C \in [0, 1]^{n \times k}$.

$$\mathbf{H}'^{(r)} = FCN(GAT^{(r)}(\hat{A}, X))$$

$$C = softmax\left(FCN\left(\sum_{r=1}^{R}\mathbf{H}'^{(r)}\right)\right) \quad (5)$$

Here $n = \frac{st}{p^2}$, and k are the number of nodes and clusters respectively.

C. Loss function

It is based on the modularity matrix B, which is defined on an undirected graph $\mathcal{G} = (\mathcal{V}, \mathcal{E})$, where $\mathcal{V} = (v_1, \ldots, v_n)$ represents the set of n nodes and $\mathcal{E} \subseteq \mathcal{V} \times \mathcal{V}$ denotes the edges. Let A be the adjacency matrix of the undirected graph $\mathcal{G}$ defined in equation (1).

The modularity matrix B is then defined as $B = A - \frac{dd^T}{2m}$, where d is the degree vector of the graph $\mathcal{G}$ and $m = |\mathcal{E}|$ represents the total number of edges. The matrix B quantifies the disparity between the actual edges in $\mathcal{G}$ and those expected in a random graph with an identical degree sequence. Positive entries in B indicate a greater density of edges within a cluster, thus enhancing the modularity score.

The modularity Q for a partition C of the graph can be computed as follows:

$$Q = \frac{1}{2m}\sum_{ij}\left[A_{ij} - \frac{d_i d_j}{2m}\right]\delta(c_i, c_j), \quad (6)$$

where c_i denotes the cluster assignment for node i, and δ is defined by the Kronecker delta function [17].

A higher modularity score signifies a more effective partitioning of the graph $\mathcal{G}$, making the maximization of Q synonymous with improved clustering. However, it has been

established that maximizing this equation is an NP-hard problem [12]. Consequently, a relaxed version of this equation expressed as:

$$\bar{Q} = \frac{1}{2m} Tr(C^T B C), \tag{7}$$

is commonly employed for optimization. Here, the cluster assignment matrix $C \in \mathbb{R}^{n \times k}$ (where n and k represent the number of nodes and clusters, respectively) is derived using equation (5). The trace operator, denoted by $Tr(\cdot)$, computes the sum of the diagonal elements of a square matrix.

We aim to cluster the resulting patch features from the ViT by minimizing the loss function $\mathcal{L}$, as delineated in [12]:

$$\mathcal{L} = -\frac{1}{2m} Tr(C^T B C) + \frac{\sqrt{k}}{n} \left\| \sum_{i=1}^{n} C_i \right\|_F - 1. \tag{8}$$

In this context, C_i denotes the soft cluster assignments for the ith node, represented as a vector of values ranging from 0 to 1 with size k. The notation $||.||_F$ refers to the Frobenius norm, which quantifies the magnitude of a matrix.

III. Experiments and Results

We employ the DINO-ViT small model [1] with a patch size of 8, and node features of size $C_{in} = 384$.

The *UnSegMedGAT* model is individually optimized for each image using the loss function $\mathcal{L}$. The initial learning rate is configured to 10^{-3} with a decay factor of 10^{-2}. We employ the ADAM [18] for the optimization of $\mathcal{L}$ in 60 epochs. Through experimentation, we find that setting the threshold parameter $\tau = 0.3$ yields improved accuracy and faster convergence across various datasets. Additionally, we explore different activation functions such as SiLU [19], SeLU [20], and ReLU [21], observing that SiLU is particularly effective for our application. As mentioned in subsection II-B, we observed best results for $R = 2$, $\{t_r\}_{r=1}^{r=R} = 2$ and $(m_1 = 128, m_2 = 64, M = 64)$.

We have also designed a collective approach in combination to regular optimization of UnSegMedGAT. Previously, model parameters are initialized and optimized separately per image without any sharing. In our approach, for first $\mathcal{T}_0$ epochs, all the images in a particular dataset will optimize with the same shared model parameters. After that for the remaining $\mathcal{T}_1$ epochs, model parameters are optimized separately for each image without any sharing. Here $\mathcal{T}_0$ and $\mathcal{T}_1$ are the free parameters. From now on, we are referring to this approach in combination to UnSegMedGAT as UnSegMedGATc.

We have considered two datasets for our experiments:1) ISIC-2018 [3] which contains dermatology images for skin cancer detection. 2) CVC-ColonDB [4] is a well-known open-access dataset for colonoscopy research. For UnSegMedGAT, we found that optimal results were achieved after 300 epochs for the ISIC2018 dataset and 60 epochs for the ColonDB dataset respectively. We observed that parameter settings of $\mathcal{T}_0 = 5$ and $\mathcal{T}_1 = 5$ for ISIC2018, as well as $\mathcal{T}_0 = 15$ and $\mathcal{T}_1 = 55$ for ColonDB, yielded improved performance for UnSegMedGATc. When comparing our UnSegMedGAT model to medical image datasets, we used the following

methods: MedSAM [2], MinCutPool [22], GDISM [23], DSM [24] and ViT-Kmeans. As shown in Table I, UnSegMedGAT outperforms state-of-the-art (SOTA) unsupervised methods. Notably, UnSegMedGAT achieves significantly better scores on ISIC-2018 compared to MedSAM. However, MedSAM performs well on CVC-ClonlonDB due to its training on large polyp datasets. On the other hand, MedSAM struggles with ISIC-2018 due to modality-imbalance issues. We also explored the impact of different activation functions on UnSegMedGAT, including SiLU, SeLU and ReLU. UnSegMedGAT with SiLU activation function yields the best results on both the medical image datasets. We evaluate the resulting segmentation masks using the Mean Intersection over Union (mIOU) score, which is based on binarized values. A higher mIOU value indicates better segmentation accuracy, with higher values indicating better performance. As illustrated in Table I, UnSegMedGAT demonstrates superior performance compared to other unsupervised methods. It achieves results on par with MedSAM for the CVC-ColonDB [4] and ISIC-2018 [3] datasets, despite MedSAM being fine-tuned on an extensive array of medical image datasets, including sizable colonoscopy datasets. However, MedSAM encounters challenges related to modality imbalance, which may explain its enhanced performance on the CVC-ColonDB dataset while resulting in significantly lower scores on the ISIC-2018 dataset. This imbalance likely arises from MedSAM's training on a larger polyp images in conjunction with smaller dermoscopy image-mask pairs.

IV. Conclusions

We proposed an unsupervised image segmentation procedure capable of combining the benefits of the attention-based features captured by a ViT, and attention coefficients capturing the inherent graph structure of the images using a Graph Attention Network. Further, we also deployed a novel collective approach to update the parameters of underlying Graph Attention network. Our experiments on the benchmark datasets show state-of-the-art results, both on ISIC-2018 and CVC-ColonDB datasets for image segmentation. The proposed model is lightweight and hence, is less prone to overfitting problems. Further, the proposed unsupervised model provides a useful way to solve various tasks in biomedical image analysis, where getting annotated data is difficult. In future work, we intend to improve the feature representation capabilities of Graph Attention Networks at the multi-hop level by incorporating generalized modularity criteria into the loss function. This strategy is anticipated to substantially enhance segmentation accuracy across medical image datasets from diverse modalities.

References

[1] M. Caron, H. Touvron, I. Misra, H. Jégou, J. Mairal, P. Bojanowski, and A. Joulin, "Emerging properties in self-supervised vision transformers," in *Proceedings of the IEEE/CVF international conference on computer vision*, 2021, pp. 9650–9660.

[2] J. Ma, Y. He, F. Li, L. Han, C. You, and B. Wang, "Segment anything in medical images," *Nature Communications*, vol. 15, no. 1, p. 654, 2024.
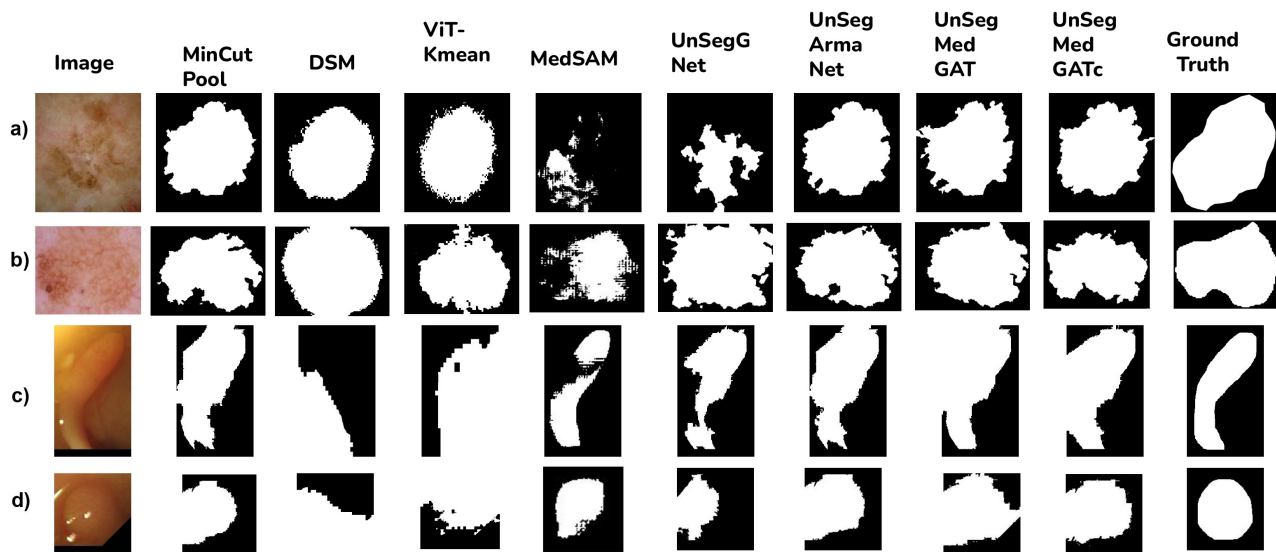
Fig. 2. Segmentation results on (a)-(b) ISIC-2018, (c)-(d) CVC-ColonDB sample images

TABLE I
AVERAGE (MIOU, DICE) SCORES FOR MEDICAL IMAGE DATA

Datasets	UnSegMedGATc	UnSegMedGAT	UnSeGArmaNet [11]	UnSegGNet [25]	MedSAM [2]	MinCutPool [22]	DSM [24]	ViT-Kmeans
ISIC-2018	(74.76,85.17)	(73.75,84.34)	(73.16,83.16)	(73.94,84.12)	(61.36,73.06)	(72.31,83.24)	(72.2,81.71)	(68.6,78.37)
ColonDB	(65.1,77.31)	(57.21,70.76)	(59.35,72.58)	(55.67,69.18)	(70.29,80.50)	(56.09,69.71)	(47.46,63.50)	(51.84,67.23)

[3] N. Codella, V. Rotemberg, P. Tschandl, M. E. Celebi, S. Dusza, D. Gutman, B. Helba, A. Kalloo, K. Liopyris, M. Marchetti *et al.*, "Skin lesion analysis toward melanoma detection 2018: A challenge hosted by the international skin imaging collaboration (isic)," *arXiv preprint arXiv:1902.03368*, 2019.

[4] J. Bernal, J. Sánchez, and F. Vilarino, "Towards automatic polyp detection with a polyp appearance model," *Pattern Recognition*, vol. 45, no. 9, pp. 3166–3182, 2012.

[5] O. Ronneberger, P. Fischer, and T. Brox, "U-net: Convolutional networks for biomedical image segmentation," in *Medical image computing and computer-assisted intervention–MICCAI 2015: 18th international conference, Munich, Germany, October 5-9, 2015, proceedings, part III 18*. Springer, 2015, pp. 234–241.

[6] V. Badrinarayanan, A. Kendall, and R. Cipolla, "Segnet: A deep convolutional encoder-decoder architecture for image segmentation," *IEEE transactions on pattern analysis and machine intelligence*, vol. 39, no. 12, pp. 2481–2495, 2017.

[7] L.-C. Chen, G. Papandreou, I. Kokkinos, K. Murphy, and A. L. Yuille, "Deeplab: Semantic image segmentation with deep convolutional nets, atrous convolution, and fully connected crfs," *IEEE transactions on pattern analysis and machine intelligence*, vol. 40, no. 4, pp. 834–848, 2017.

[8] T. N. Kipf and M. Welling, "Semi-supervised classification with graph convolutional networks," *arXiv preprint arXiv:1609.02907*, 2016.

[9] K. Han, Y. Wang, J. Guo, Y. Tang, and E. Wu, "Vision gnn: An image is worth graph of nodes," *Advances in neural information processing systems*, vol. 35, pp. 8291–8303, 2022.

[10] A. Aflalo, S. Bagon, T. Kashti, and Y. Eldar, "Deepcut: Unsupervised segmentation using graph neural networks clustering," in *Proceedings of the IEEE/CVF International Conference on Computer Vision*, 2023, pp. 32–41.

[11] K. S. G. Reddy, B. Saran, A. M. Adityaja, S. J. Shigwan, N. Kumar, and S. Mukherjee, "Unsegarmanet: Unsupervised image segmentation using graph neural networks with convolutional arma filters," 2024. [Online]. Available: https://arxiv.org/abs/2410.06114

[12] A. Tsitsulin, J. Palowitch, B. Perozzi, and E. Müller, "Graph clustering with graph neural networks," *Journal of Machine Learning Research*, vol. 24, no. 127, pp. 1–21, 2023.

[13] M. E. Newman, "Modularity and community structure in networks," *Proceedings of the national academy of sciences*, vol. 103, no. 23, pp. 8577–8582, 2006.

[14] A. Vaswani, "Attention is all you need," *Advances in Neural Information Processing Systems*, 2017.

[15] P. Velickovic, G. Cucurull, A. Casanova, A. Romero, P. Lio, and Y. Bengio, "Graph attention networks," *International Conference on Learning Representations*, 2018.

[16] J. T. Barron and B. Poole, "The fast bilateral solver," in *European conference on computer vision*. Springer, 2016, pp. 617–632.

[17] D. Kozen and M. Timme, "Indefinite summation and the kronecker delta," *Cornell University Library*, 2007.

[18] D. P. Kingma and J. Ba, "Adam: A method for stochastic optimization," *arXiv preprint arXiv:1412.6980*, 2014.

[19] S. Elfwing, E. Uchibe, and K. Doya, "Sigmoid-weighted linear units for neural network function approximation in reinforcement learning," *Neural networks*, vol. 107, pp. 3–11, 2018.

[20] P. Ramachandran, B. Zoph, and Q. V. Le, "Searching for activation functions," *arXiv preprint arXiv:1710.05941*, 2017.

[21] X. Glorot, A. Bordes, and Y. Bengio, "Deep sparse rectifier neural networks," in *Proceedings of the fourteenth international conference on artificial intelligence and statistics*. JMLR Workshop and Conference Proceedings, 2011, pp. 315–323.

[22] F. M. Bianchi, D. Grattarola, and C. Alippi, "Spectral clustering with graph neural networks for graph pooling," in *International conference on machine learning*. PMLR, 2020, pp. 874–883.

[23] M. Trombini, D. Solarna, G. Moser, and S. Dellepiane, "A goal-driven unsupervised image segmentation method combining graph-based processing and markov random fields," *Pattern Recognition*, vol. 134, p. 109082, 2023.

[24] L. Melas-Kyriazi, C. Rupprecht, I. Laina, and A. Vedaldi, "Deep spectral methods: A surprisingly strong baseline for unsupervised semantic segmentation and localization," in *Proceedings of the IEEE/CVF Conference on Computer Vision and Pattern Recognition*, 2022, pp. 8364–8375.

[25] K. S. G. Reddy, B. Saran, A. M. Adityaja, S. J. Shigwan, and N. Kumar, "Unseggnet: Unsupervised image segmentation using graph neural networks," *arXiv preprint arXiv:2405.06057*, 2024.